Article

Electric Field Effects on Photoluminescence of CdSe Nanoparticles in a PMMA Film

Takakazu Nakabayashi [†], Ruriko Ohshima and Nobuhiro Ohta *

Research Institute for Electronic Science (RIES), Hokkaido University, Sapporo 001-0020, Japan;
E-Mails: takan@es.hokudai.ac.jp (T.N.); rohshima@es.hokudai.ac.jp (R.O.)

[†] Current address: Graduate School of Pharmaceutical Sciences, Tohoku University, Aoba-ku, Sendai 980-8578, Japan; E-Mail: takan@m.tohoku.ac.jp.

* Author to whom correspondence should be addressed; E-Mail: nohta@es.hokudai.ac.jp; Tel.: +81-11-706-9410; Fax: +81-11-706-9406.

Abstract: External electric field effects on spectra and decay of photoluminescence (PL) as well as on absorption spectra were measured for CdSe nanoparticles in a poly(methyl methacrylate) (PMMA) film. Electrophotoluminescence (E-PL) spectra as well as electroabsorption spectra show a remarkable Stark shift which depends on the particle size, indicating a large electric dipole moment in the first exciton state. The E-PL spectra also show that PL of CdSe is quenched by application of electric fields, and the magnitude of the field-induced quenching becomes larger with increasing size. The PL decay profiles observed in the absence and presence of electric field show that the field-induced quenching of PL mainly originates from the field-induced decrease in population of the emitting state prepared through the relaxation from the photoexcited state.

Keywords: CdSe; electric field effects; photoluminescence; field-induced quenching

1. Introduction

Semiconductor nanoparticles in size of 2–6 nm show quantum size effects in optical properties, that is, the absorption and photoluminescence (PL) bands shift to higher energy with reducing grain size. Such nanoparticles have been proposed for applications of laser source, bioimaging, and solar energy

conversion, with their special optical properties of high PL yields and tunability of absorption and PL wavelengths [1–5]. A large number of theoretical and experimental studies have been devoted to examine the optical properties of nanometer-sized materials [6–9]. However, the mechanism of the strong PL generation is still unresolved, and preparation of high-luminescent nanoparticles is a subject of investigation.

Measurements of external electric field effects on absorption and PL spectra are useful to examine electronic structures and photoexcitation dynamics of molecules and molecular systems [10–12]. We measured the so-called electroabsorption and electrophotoluminescence spectra (plots of the electric-field-induced change in absorption and PL intensity as a function of wavelength or wavenumber) to investigate molecular properties including intramolecular and intermolecular electron transfer [13–15], excimer formation [16], photoisomerization [17], and electrostatic interaction in protein [18]. Measurements of these spectra provide unique information about the differences in electric dipole moment (**μ**) and molecular polarizability (**α**) between the ground state and excited states. These spectra have also been used to probe field-induced molecular orientation [19,20], to examine the stability of organic light-emitting diode materials [21], and to examine the efficiency of dye-sensitized solar cells [22].

Cadmium selenide (CdSe) nanoparticle is one of the semiconductor nanoparticles that have been widely studied and proposed for optoelectronic and biomedical applications [1–5,23–25]. In the present study, we measured electrophotoluminescence spectra and field-induced change in the PL decay profile of CdSe nanoparticles in a poly(methyl methacrylate) (PMMA) film, to examine the Stark shift of the PL spectra and the electric field effects on photoexcitation dynamics. The PL intensity depends on the absorption intensity, and so the field-induced change in absorption intensity must be known in order to discuss the field effect on photoexcitation dynamics on the basis of the electrophotoluminescence spectra and the field-induced change in PL decay profile. Therefore, electroabsorption spectra were also measured under the same experimental conditions with which the field-induced change in PL intensity is measured, although the electroabsorption spectra of CdSe nanoparticles had been already reported by Alivisatos and his co-workers [26,27] and Bawendi and his co-workers [28]. We applied external electric fields up to 0.5 MV cm^{-1} on absorption, PL, and PL decay profile of CdSe nanoparticles. We compared the present results with those of CdS and CdTe nanoparticles which we had previously reported [29–32]. Hereafter, electroabsorption and electrophotoluminescence spectra are abbreviated as E-A and E-PL spectra, respectively, and applied electric field is denoted by *F*.

2. Results and Discussion

2.1. Theory

E-A spectrum, *i.e.*, plots of the field-induced change in absorbance ($\Delta A(v)$) as a function of wavenumber, for an isotropic sample in rigid matrices such as PMMA is generally given by a sum of the zeroth, first, and second derivatives of the absorption spectrum $A(v)$ as follows [10–12]:

$$\Delta A(v) = (fF)^2 \left[A_\chi A(v) + B_\chi v \frac{d}{dv}\left\{\frac{A(v)}{v}\right\} + C_\chi v \frac{d^2}{dv^2}\left\{\frac{A(v)}{v}\right\} \right] \tag{1}$$

in which $F = |\boldsymbol{F}|$, and f is the internal field factor. The coefficient A_χ depends on the transition polarizability, and B_χ and C_χ are given by the following equations:

$$B_\chi = \frac{\Delta\bar{\alpha}}{2hc} + \left\{ \frac{(\Delta\alpha_m - \Delta\bar{\alpha})(3\cos^2\chi - 1)}{10hc} \right\} \quad (2)$$

$$C_\chi = (|\Delta\boldsymbol{\mu}|)^2 \left\{ \frac{5 + (3\cos^2\chi - 1)(3\cos^2\eta - 1)}{30h^2c^2} \right\} \quad (3)$$

where $\Delta\boldsymbol{\mu}$ and $\Delta\boldsymbol{\alpha}$ are the differences in electric dipole moment and molecular polarizability, respectively, between the ground state (g) and the excited state (e), *i.e.*, $\Delta\boldsymbol{\mu} = \boldsymbol{\mu}_e - \boldsymbol{\mu}_g$ and $\Delta\boldsymbol{\alpha} = \boldsymbol{\alpha}_e - \boldsymbol{\alpha}_g$. $\Delta\bar{\alpha}$ denotes the trace of $\Delta\boldsymbol{\alpha}$. $\Delta\alpha_m$ is the diagonal component of $\Delta\boldsymbol{\alpha}$ with respect to the direction of the transition dipole moment; χ is the angle between $\boldsymbol{F}$ and the electric vector of the light; and η is the angle between $\Delta\boldsymbol{\mu}$ and the transition dipole moment.

It is also expected that E-PL spectra can be given by a sum of the zeroth, first, and second derivatives of the corresponding PL spectra, as in the case of E-A spectrum. In immobilized sample, the first and second derivative components can be presented similarly as Equations (2) and (3), respectively, giving the information about the change in polarizability and electric dipole moment, respectively, between the emitting state and the ground state. In contrast with the E-A spectra, further, the zeroth derivative contribution will give information on how the excitation dynamics following excitation is affected by application of electric field. In order to discuss the field effects on excitation dynamics, however, not only the measurements of the E-PL spectra but also the E-A measurements are necessary since the field-induced change in absorbance, which is not related to the change in dynamics, induces a change in PL intensity, as mentioned already.

2.2. Electric Field Effects on Absorption (E-A Measurements)

Before the E-PL measurements, absorption and E-A spectra were always measured in every case. Figure 1 shows the E-A spectra thus obtained for different sizes of CdSe nanoparticle in a PMMA film. Note that the magic angle of $\chi = 54.7°$ was used for the measurements of the E-A spectra shown in Figure 1. Each absorption spectrum exhibits structures, and the shoulder observed in the low wavenumber region is assigned to the transition to the first exciton state. As the particle size increases, the peak position of the absorption band assigned to the transition to the first exciton state shifts to a longer wavelength, due to the quantum size effect. Hereafter, the absorption band resulting from the transition to the first exciton state is named as the first exciton band. As shown in Figure 1, the field-induced change is remarkable around the first exciton band, indicating that absorption bands to higher exciton states do not show significant field effects; the observed E-A spectra are dominated by the field-induced change in the transition to the first exciton state. All the E-A spectra around the first exciton band are similar in shape to the second derivative of the first exciton band, as already reported [26–28].

As expected from Equation (1), the magnitude of the field-induced change in absorption intensity was proportional to the square of applied field strength (see Figure 2). The fact that the shape of the E-A spectrum is similar to the second derivative spectrum suggests that the field-induced change in absorption intensity comes from the change in $|\Delta\boldsymbol{\mu}|$ following the transition to the first exciton state. To

perform the detailed analysis of the E-A spectra, the first exciton band was extracted by subtraction of the base profile from the observed absorption spectrum, and the E-A spectrum was simulated with a sum of the zeroth, first, and second derivative spectra of the extracted first exciton band. Figure 3 shows the first and second derivative spectra of the extracted first exciton band of CdSe nanoparticles with a diameter of 2.1 nm, as an example of the simulation. The base profile was obtained by fitting the absorption spectrum with a polynomial function on the assumption that the base exhibits a smooth profile in the whole spectral region of the measured spectrum. As shown in Figure 1, all the E-A spectra could be fitted by the second derivative of the first exciton band, but the small contribution of the first derivative spectrum was necessary to reproduce the E-A spectra of CdSe with a diameter of 2.1 and 2.5 nm. It should be also noted that the E-A spectra were fitted when the absorption profile of the first exciton band was assumed to be a Gaussian [30,32]. The coefficient A_χ of Equation (1) is negligible in all the E-A spectra, indicating that the field-induced change in transition dipole moment to the first exciton state is negligibly small in the CdSe nanoparticles. The fact that the E-A spectra observed at the magic angle of χ and at $90°$ are nearly the same also indicates that the CdSe nanoparticles are fixed in PMMA even with the applied electric fields.

Figure 1. Electroabsorption (E-A) spectra (shaded line) and absorption spectra (solid line) of CdSe nanoparticles of average diameter of (**a**) 2.1, (**b**) 2.5, (**c**) 3.3, (**d**) 5.0, and (**e**) 6.6 nm in a poly(methyl methacrylate) (PMMA) film. The simulated E-A spectra are also shown by a dotted line. Applied field strength was 0.4 MV cm^{-1} in every case.
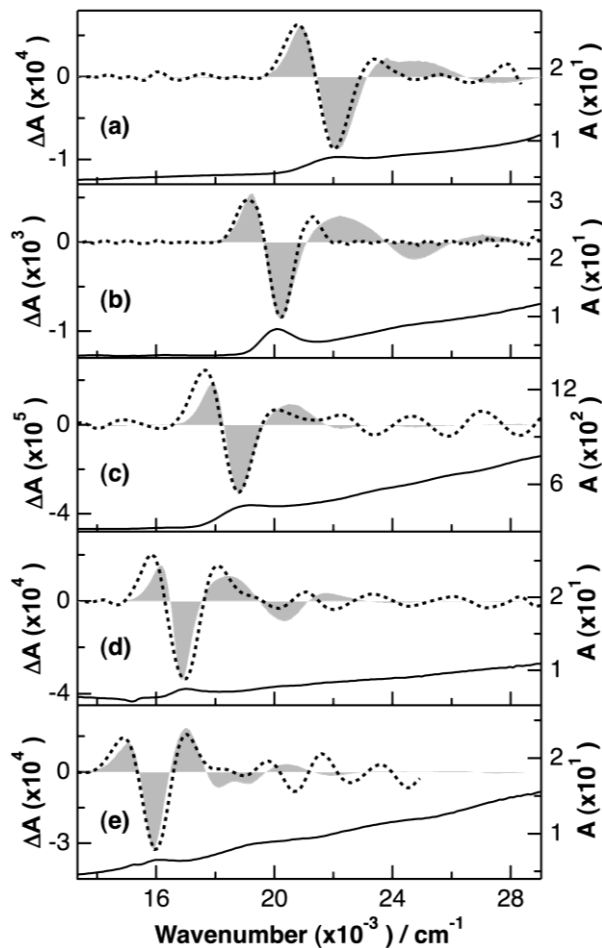
Figure 2. Plots of the E-A intensity of CdSe nanoparticles with a diameter of 2.5 nm in a PMMA film as a function of the square of the applied electric field. The intensity was monitored at 495 nm.
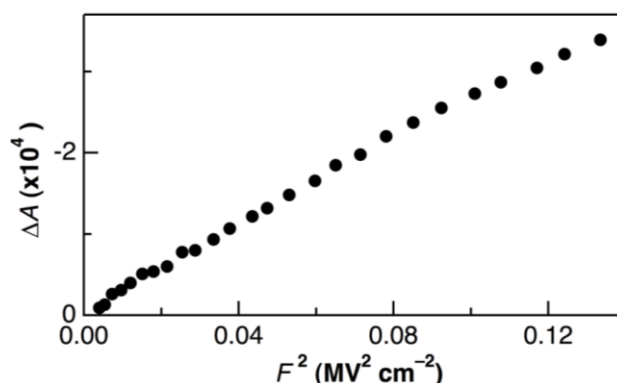

Figure 3. Simulation of the E-A spectrum of CdSe nanoparticles with a diameter of 2.1 nm in a PMMA film. (**a**) The absorption spectrum (solid line) and the base function (dotted line) used for the extraction of the first exciton band; (**b**) The first derivative (dotted line) and second derivative (solid line) spectra of the extracted first exciton band; (**c**) The E-A spectrum (shaded line) and the simulated one (dotted line). Applied field strength was 0.4 MV cm^{-1}.
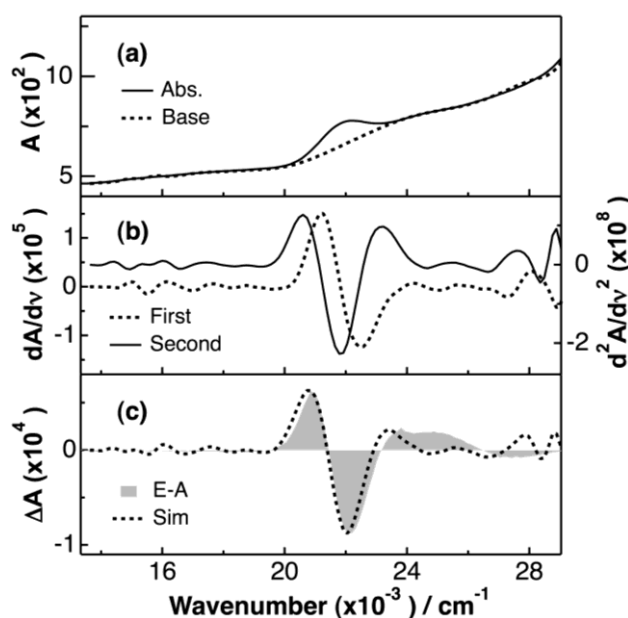
The magnitude of $\Delta\mu$ between the first exciton state and the ground state was obtained by the evaluation of the second derivative part in the E-A spectrum. The size dependence of the obtained $|\Delta\mu|$ is shown in Figure 4. Note that the value of $3\cos^2\chi - 1$ in Equation (3) becomes zero because of the E-A measurements at the magic angle of $\chi = 54.7°$. The local field was assumed to be the same as the applied electric field, *i.e.*, $f = 1$. All the CdSe nanoparticles exhibit a large value of $|\Delta\mu|$ following the transition to the first exciton state, indicating that the CdSe nanoparticles have large CT character in the first exciton state, that is, the electric dipole moment in the first exciton state is expected to be much larger than that in the ground state.

Figure 4. Plots of the magnitude of difference in electric dipole moment (Δ**μ**) between the first exciton state and the ground state of CdSe nanoparticles in a PMMA film as a function of particle size. Each error bar represents the mean ± standard deviation for values from several measurements.
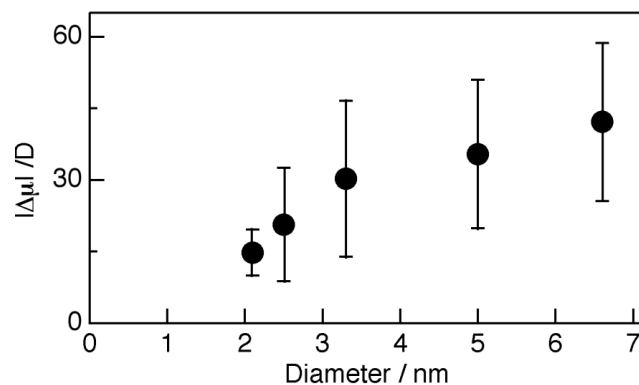
As shown in Figure 4, there is a clear tendency that the |Δ**μ**| value increases with an increase in the particle size, indicating that the dipole moment of the CdSe nanoparticle in the first exciton state becomes larger as the particle size increases. The present result is consistent with the one reported previously [26,27]. The significant increase in |Δ**μ**| with increasing particle size was also observed for CdS nanoparticles in a PMMA film [30]. On the other hand, the CdTe nanoparticles exhibited different behavior in a poly(vinyl alcohol) (PVA) film: the |Δ**μ**| value remains unchanged with particle size in the region of 2–4 nm, and slight increase in |Δ**μ**| with increasing particle size was observed with diameters larger than 4 nm [32]. It has also been reported that the first exciton band gives the second derivative shape in the E-A spectra of PbS and PbSe [33,34].

It has been suggested that the polar excited state is not necessary to interpret the E-A spectra of CdSe nanoparticles and that the second derivative component results from the allowed excited state and dark states which are coupled by the electric field and have overlapping transitions [28]. However, the fact that the second derivative shape is observed in the exciton state of not only CdSe nanocrystals but also in other semiconductor nanocrystals including CdS, CdTe, PbSe and PbS seems to show that the second derivative component comes from the inherent properties of nanocrystals, and not from the accidental overlap of the allowed transition band and the forbidden transition band. Further, wurtzite CdSe nanocrystals have been reported to have a large electric dipole moment which increases with an increase in the size, that is, 41 D for 2.7 nm diameter and 98 D for 5.6 nm [35]. Therefore, it is not strange to find out that the electric dipole moment increases as the nanocrystal is excited to the exciton state.

2.3. Electric Field Effects on Photoluminescence (E-PL Measurements)

E-PL spectra have been measured for different sizes of CdSe nanoparticles in a PMMA film, together with the PL spectra. The results are shown in Figure 5. Excitation was done at the wavelength where the field-induced change in absorption intensity was negligible. This could be done because E-A spectra were measured under the same experimental conditions, as mentioned above. Therefore, the change in PL intensity coming from the field-induced change in absorption intensity can be neglected.

The narrow PL band located in the wavenumber region just lower than the first exciton band arises from the exciton-emitting state, while another broad PL band located in the much lower wavenumber region, which was clearly observed with a small diameter of 2.1 nm, is assigned to the emission from trap states arising from surface atoms to the ground state [36]. Hereafter, the narrow and broad emissions are named as exciton emission and trap emission, respectively. It is noted that these two emissions shift to a longer wavelength, as the particle size increases (see Figure 5), as in the case of the first exciton band.

> **Figure 5.** Electrophotoluminescence (E-PL) spectra (shaded line) and photoluminescence (PL) spectra (solid line) of CdSe nanoparticles of average diameter of (**a**) 2.1, (**b**) 2.5, (**c**) 3.3, (**d**) 5.0, and (**e**) 6.6 nm in a PMMA film. The simulated E-PL spectra are also shown by a dotted line. Excitation wavelength was was (**a**) 379, (**b**) 380, (**c**) 390, (**d**) 400, and (**e**) 400 nm. Applied field strength was 0.4 MV cm^{-1} in every case.
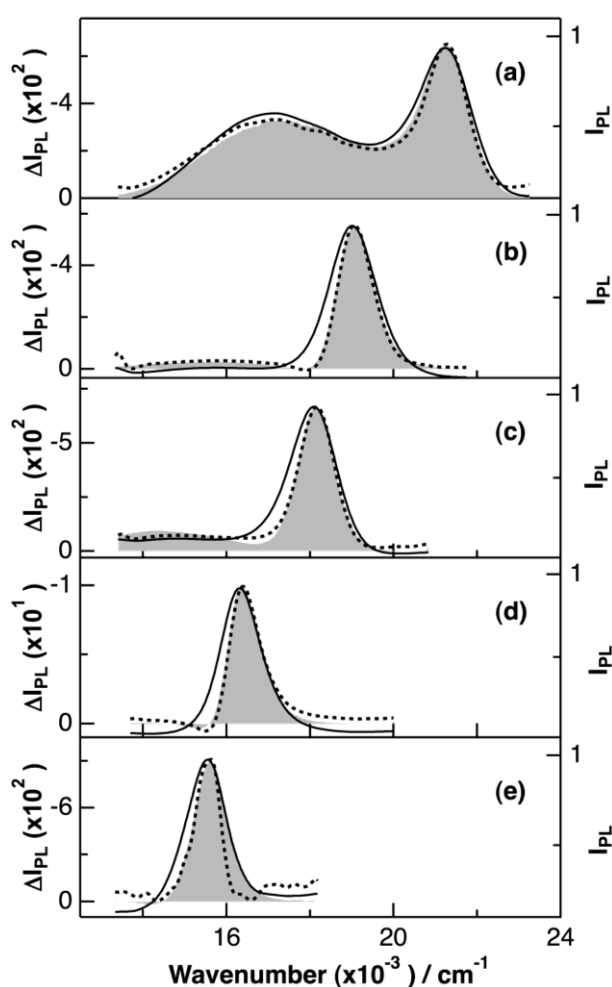
In all the E-PL spectra, field-induced quenching of PL is predominantly observed. It is expected that E-PL spectra are reproduced by a superposition of the PL spectrum and its first and second derivative spectra. In the observed E-PL spectra, the presence of the second derivative contribution can be explained from the result that the bandwidth of the E-PL spectra of the exciton emission is smaller than that of the exciton emission in the PL spectrum. The contribution of the first derivative is known from the result that the peak position of the E-PL spectra of the exciton emission is slightly

blue-shifted from the peak of the PL spectrum. In fact, the E-PL spectra of the exciton emission could be reproduced by a linear combination of the zeroth, first and second derivatives of the exciton emission, as shown in Figure 5. Note that the trap emission was assumed to be only quenched by application of *F*, *i.e.*, with only the zeroth derivative component. One example of the simulation is shown in Figure 6, together with the first and second derivatives of the exciton emission spectrum, for CdSe nanoparticles having a diameter of 5.0 nm. To evaluate the magnitude of the field-induced quenching, the intensity of the E-PL spectrum was integrated across the whole spectral region since the derivative components do not give a change in total intensity. The magnitudes of $\Delta\boldsymbol{\mu}$ were estimated from the analysis of the E-PL spectra by assuming that $f = 1$ and that the second term of Equation (3) is negligible. The results are shown in Figure 7. As already mentioned, the field-induced change in emission intensity, $\Delta I_{PL}(\nu)$, is given by a linear combination of the zeroth, first and second derivatives of the PL spectrum and the coefficient of the second derivative is given by Equation (3), as in the case of $\Delta A(\nu)$. The $|\Delta\boldsymbol{\mu}|$ value between the exciton-emitting state and the ground state is estimated to be around 30–60 D with diameter of 2.1–6.6 nm, with a trend that $|\Delta\boldsymbol{\mu}|$ increases with increasing particle size, as in the case for the values determined from the E-A spectra. The blue shift of the E-PL spectrum in comparison with the corresponding exciton PL band (see Figure 5) means that the polarizability in the exciton-emitting state is larger than that in the ground state. Note that E-PL spectra having inverted scale of intensity are compared with the PL spectra in Figures 5 and 6 and that a similar shift was observed in CdTe nanoparticles [32].

Figure 6. Simulation of the E-PL spectrum of CdSe nanoparticles with a diameter of 5.0 nm in a PMMA film. (**a**) The E-PL spectrum (shaded line) and the corresponding PL spectrum (dotted line); (**b**) The first derivative (dotted line) and second derivative (solid line) spectra of the PL spectrum shown in (a); (**c**) The E-PL spectrum (shaded line) and the simulated one (dotted line). Applied field strength was 0.4 MV cm^{-1}.
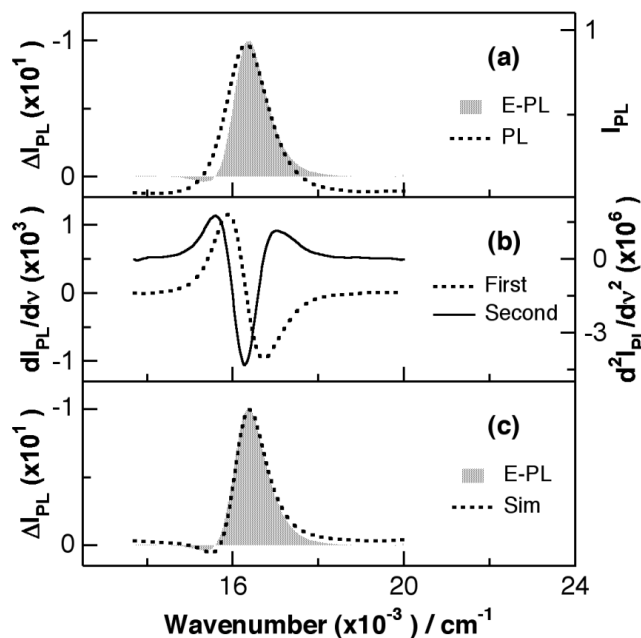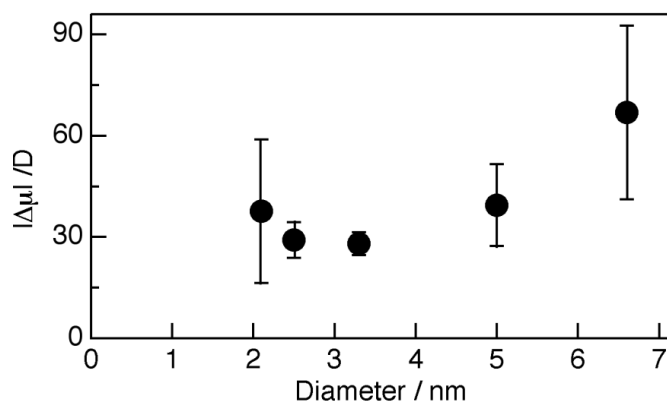
Figure 7. Plots of the magnitude of Δ**μ** between the exciton-emitting state and the ground state of CdSe nanoparticles in a PMMA film as a function of particle size. Each error bar represents the mean ± standard deviation for values from several measurements.

The size dependence of the field-induced quenching is shown in Figure 8. When the PL yield at zero field and its field-induced change are denoted by ϕ and Δϕ, respectively, the field-induced change in PL yield relative to the total yield is given by Δϕ/ϕ. As shown in Figure 8, the |Δϕ/ϕ| value appears to increase slightly, as the size increases. It should be noted that the magnitude of Δϕ/ϕ was as large as around 10% for CdSe nanoparticles with a diameter of 5.0 or 6.6 nm in the presence of 0.4 MV cm^{-1}. In the present experiments, the quantum yield of PL was not measured for each sample, but it is considered that ϕ depends on the surface structures of nanocrystals, and this comes from different interactions between nanocrystal and surrounding matrix. This is supported by the emission decay measurements which will be shown later. As the size becomes larger, the surface area becomes larger, which may increase the fluctuation of ϕ. This kind of fluctuation of ϕ may increase the fluctuation of Δϕ/ϕ as well. Therefore, a large fluctuation of Δϕ/ϕ may arise from the variety in surface structure of the sample. Even so, the trend observed in Figure 8, that is, the nearly monotonic increase of Δϕ/ϕ with increasing diameter of nanocrystals seems to be essential.

Figure 8. Plots of the field-induced PL quenching relative to the total PL intensity of CdSe nanoparticles in a PMMA film as a function of diameter of nanoparticles. Applied field strength was 0.4 MV cm^{-1}. Each error bar represents the mean ± standard deviation for values from several measurements.
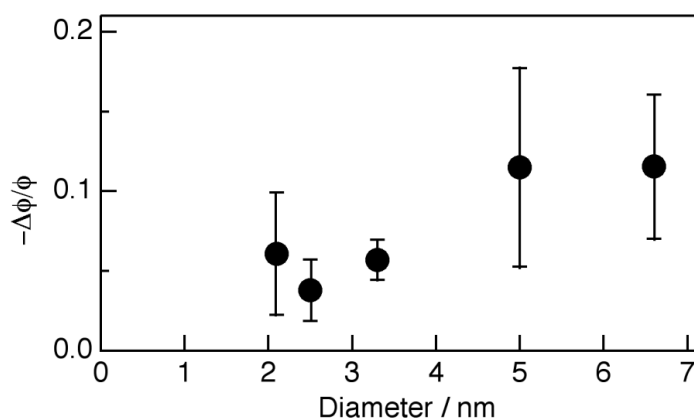
From the steady state measurements, it was difficult to confirm whether the field-induced change in PL intensity is ascribed to a change in PL lifetime or a change in initial population of the emitting state. Following this, we measured electric field effects on the PL decay of the CdSe nanoparticles. If the lifetime is not affected by F, the ratio of the decay profile in the presence of F relative to that in the absence of F is constant in the whole time region. If the population of the emitting state is reduced or enhanced by F, on the other hand, the ratio between those decay profiles should not be unity at the initial stage of time. Figure 9a shows the representative PL decays of the CdSe nanoparticles with a diameter of 6.6 nm in PMMA in the presence and absence of F. The monitoring PL wavelength was 640 nm, which arises from the exciton-emitting state. As mentioned in the Experimental Section, these decays were stored in turn with time duration of 30 ms and the accumulation time was several hours, so that the field-induced change in absolute intensity as well as the decay constant could be properly evaluated [37]. It is shown in Figure 9a that the PL decay is different between the presence and absence of F. Figure 9b,c show the difference between the decays observed at zero field ($I_0(t)$) and at 0.5 MV cm^{-1} ($I_{PL}(t)$), i.e., $I_{PL}(t) - I_0(t)$, referred to as $\Delta I_{PL}(t)$, and the ratio $I_{PL}(t)/I_0(t)$, respectively. The value of $\Delta I_{PL}(t)$ in Figure 9b is negative during the full decay, showing that the PL intensity is quenched in the presence of F in the whole time region. It should be noted in Figure 9c that the magnitude of $I_{PL}(t)/I_0(t)$ is smaller than unity even just after photoexcitation, indicating that the initial population of the exciton-emitting state following photoexcitation is reduced in the presence of F. All the time profiles of $I_0(t)$, $I_{PL}(t)$, $\Delta I_{PL}(t)$, and $I_{PL}(t)/I_0(t)$ were fitted by assuming a tetraexponential decay, i.e., $\Sigma_i A_i \exp(-t/\tau_i)$, where A_i and τ_i denote the pre-exponential factor and the PL lifetime of component i, respectively. The representative lifetime and the pre-exponential factor of each component in the absence of F were evaluated to be as follows: $\tau_1 = 0.08$ ns, $\tau_2 = 1.18$ ns, $\tau_3 = 5.13$ ns, $\tau_4 = 25.11$ ns, $A_1 = 0.764$, $A_2 = 0.156$, $A_3 = 0.069$, $A_4 = 0.011$. The corresponding values in the presence of 0.5 MV cm^{-1} were as follows: $\tau_1 = 0.08$ ns, $\tau_2 = 1.17$ ns, $\tau_3 = 5.13$ ns, $\tau_4 = 24.86$ ns, $A_1 = 0.648$, $A_2 = 0.136$, $A_3 = 0.053$, $A_4 = 0.009$. The sum of the pre-exponential factors in the absence of F was normalized to unity in this evaluation.

The multi-exponential behavior in the PL decay probably arises from inhomogeneous environments in a PMMA film, i.e., the presence of different interactions between the coated materials and PMMA which show different PL lifetimes from each other [38]. It must be confessed that lifetimes as well as pre-exponential factors of different samples are not always identical with each other, which may arise from photoenhancement of PL of the nanoparticle-doped polymer films [39–42]. The magnitude of A_i corresponds to the population of each emitting state, and the ratio of $\Sigma_i A_i$ at 0.5 MV cm^{-1} to that at zero field is 0.85. This result indicates that the field-induced decrease in initial population of the exciton-emitting state causes the decrease in PL intensity in the presence of F in Figure 8. From the present E-A spectra in Figures 1 and 3, it is shown that the CdSe nanoparticles in the first exciton state have large CT character. Thus, the observed field-induced decrease in initial population of the exciton-emitting state suggests that the field-assisted charge separation into hole and electron occurs from the first exciton state in competition with the relaxation to the exciton-emitting state; i.e., the formation of the exciton-emitting state is reduced by application of F. The significant field-induced decrease in initial population was also confirmed in the PL decay profile of the CdSe nanoparticles with a diameter of 3.3 nm. The average PL lifetime, defined by $\Sigma_i A_i \tau_i / \Sigma_i A_i$, was estimated to be 0.88 ns at zero field and 0.84 ns at 0.5 MV cm^{-1} for the CdSe nanoparticles with a diameter of 6.6 nm. If a

well-passivated CdSe having a much longer lifetime is used, there may be a possibility that the electric field effect in the fluorescence lifetime is much larger than the one observed in the present experiments. The decrease in average PL lifetime observed in the present experiments mainly results from the change in the ratio among the pre-exponential factors in the presence of F. The slight field-induced decrease in τ_2 and τ_4 suggests that the nonradiative process at the exciton-emitting state is accelerated by F. The non-radiative process from the exciton-emitting state is considered to be the formation of surface trap states undergoing further non-radiative decays [30,32,40], suggesting the field-induced enhancement of the trap state formation process. Since the population of the exciton state from the photoexcited state is markedly reduced by the application of electric fields, the population of the trap state also becomes smaller in the presence of an electric field, even when the formation yield of the trap state from the exciton state is a little enhanced by electric fields. In the results, the field-induced quenching of both the exciton emission and the trap emission was observed.

Figure 9. (**a**) Decay profiles of PL of CdSe nanoparticles with a diameter of 6.6 nm in a PMMA film at zero field (blue line) and at 0.5 MV cm^{-1} (black line); (**b**) The difference between the decays observed at 0.5 MV cm^{-1} and at zero field (black line), together with the simulated difference (red line) and the decay at zero field (blue line); (**c**) The ratio of the decay observed at 0.5 MV cm^{-1} to that at zero field (black line), together with the simulated one (red line). The excitation wavelength and the PL monitoring wavelengths were 400 and 640 nm, respectively.
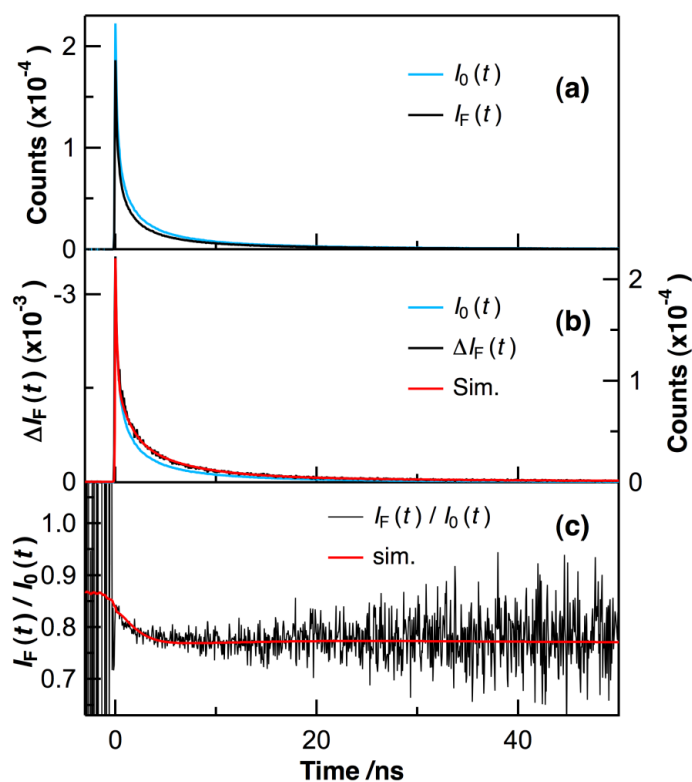
The field-induced quenching of both exiton emission and trap emission are also observed in other semiconductor nanocrystals, *i.e.*, in CdS and CdTe nanocrystals embedded in a PMMA film [30–32]. In those nanocrystals, the field-induced quenching of PL is also ascribed to the field-induced decrease

of the population of the emitting state from the photoexcited state, because the initial intensity just following photoexcitation remarkably decreases in the presence of *F*. The present results may suggest that the exciton state of CdSe nanocrystals regarded as a charge-separated state in nature is separated into the hole and electron within each nanoparticle by application of electric fields. The field effect on PL intensity observed in CdSe, as well as in CdS and CdTe, seems to be common in semiconductor nanocrystals.

Gurinovich *et al.* [43] also measured electric field effects on absorption and photoluminescence of CdSe nanoparticles with a diameter of 4 nm in PMMA and reported the tremendous decreases both in the absorption intensity at the exciton peak and in the photoluminescence intensity by the application of 0.2 MV cm^{-1}. Such remarkable decreases both in PL intensity and in absorption intensity were not observed in the present E-A and E-PL measurements.

3. Experimental Section

E-PL spectra and E-A spectra were measured by the same system and procedures as reported elsewhere [13–22]. PMMA (*MW* = 120,000) was obtained from Aldrich and purified by a precipitation with a mixture of benzene and methanol. CdSe nanoparticles with average diameters of 2.1, 2.5, 3.3, 5.0, and 6.6 nm [44] were purchased from Aldrich (Lumidot™, St. Louis, MO, USA). The particles were coated with hexadecylamine (2.1, 2.5, and 3.3 nm) or hexadecylamine/trioctylphosphine oxide (5.0 and 6.6 nm). A PMMA film containing CdSe nanoparticles was prepared by a spin coating method on an indium-tin-oxide (ITO) coated quartz substrate. Then, a semitransparent aluminum (Al) film was deposited on the dried polymer film by a vacuum vapor deposition technique. The ITO and Al films were used as electrodes. The concentration of CdSe nanoparticles in PMMA was so low that the energy transfer between different nanocrystals could not be expected.

All the measurements were performed at room temperature. A sinusoidal ac voltage was applied to the sample polymer films, and field-induced change in absorption intensity or PL intensity was detected with a lock-in amplifier at the second harmonic of the modulation frequency. A dc component of the transmitted light intensity or the PL intensity was simultaneously observed. The angle between *F* and the electric vector of the excitation light was set to be 54.7 ° (magic angle) in the E-A measurements [45], and depolarized PL was detected in the E-PL measurements. Applied field strength was evaluated from the applied voltage divided by the thickness.

Time-resolved PL measurements in the presence and absence of *F* were carried out by a single-photon counting lifetime measurement system combined with a pulse generator supplying a bipolar square wave [37]. Briefly, the excitation light source was a second harmonic of the output from a mode-locked femtosecond Ti:sapphire laser (Tsunami, Spectra Physics, Santa Clara, CA, USA). The repetition rate was selected to be ~3.7 MHz with a pulse picker (model 350–160, Conoptics, Danbury, CT, USA) from the original 81 MHz. PL from the sample was dispersed with a monochromator (G-250, Nikon, Tokyo, Japan) and detected with a microchannel-plate photomultiplier (R3809U-52, Hamamatsu Photonics, Hamamatsu, Japan). PL signals were discriminated and then led to a time-to-amplitude converter. Applied voltage was a repetition of rectangular waves of positive, zero, negative, and zero bias in turn, and the time duration of each bias was 30 ms. Four different decay profiles corresponding to positive, zero, negative, and zero sample bias, respectively, were stored in each of the different

memory-segments of a multichannel pulse height analyzer (7700, SEIKO EG&G, Tokyo, Japan). The instrumental response function had a width of ~60 ps (FWHM).

4. Conclusions

The E-A and E-PL spectra of CdSe nanoparticles were measured in a PMMA film. The analysis of both the E-A spectra and the E-PL spectra indicates a large electric dipole moment in the first exciton state, which is much larger than that in the ground state. The difference of the dipole moment between the first exciton state and the ground state becomes larger with increasing particle size. Electric-field-induced quenching is dominant in the E-PL spectra, which arises from reduction of the population of the exciton-emitting state following photoexcitation in the presence of F. The magnitude of the field-induced quenching becomes larger for CdSe nanoparticles with larger diameters of 5.0 and 6.6 nm.

Author Contributions

Takakazu Nakabayashi assisted the experiments and analyzed the data, and co-wrote the manuscript. Ruriko Ohshima carried out the experiments and analyzed the majority of the data. Nobuhiro Ohta conceived and conducted the research, and checked the analysis and wrote the manuscript.

Conflicts of Interest

The authors declare no conflict of interest.

References

1. Medintz, I.L.; Uyeda, H.T.; Goldman, E.R.; Mattoussi, H. Quantum dot bioconjugates for imaging, labelling and sensing. *Nat. Mater.* **2005**, *4*, 435–446.
2. Wang, X.; Ren, X.; Kahen, K.; Hahn, M.A.; Rajeswaran, M.; Maccagnano-Zacher, S.; Silcox, J.; Cragg, G.E.; Efros, A.L.; Krauss, T.D. Non-blinking semiconductor nanocrystals. *Nature* **2009**, *459*, 686–689.
3. Li, J.; Zhang, J.Z. Optical properties and applications of hybrid semiconductor nanomaterials. *Coord. Chem. Rev.* **2009**, *253*, 3015–3041.
4. Regulacio, M.D.; Han, M.-Y. Composition-tunable alloyed semiconductor nanocrystals. *Acc. Chem. Res.* **2010**, *43*, 621–630.
5. Frasco, M.F.; Chaniotakis, N. Bioconjugated quantum dots as fluorescent probes for bioanalytical applications. *Anal. Bioanal. Chem.* **2010**, *396*, 229–240.
6. Henglein, A. Small-particle research: Physicochemical properties of extremely small colloidal metal and semiconductor particles. *Chem. Rev.* **1989**, *89*, 1861–1873.
7. Alivisatos, P. The use of nanocrystals in biological detection. *Nat. Biotechnol.* **2004**, *22*, 47–52.
8. Lakowicz, J.R. Plasmonics in biology and plasmon-controlled fluorescence. *Plasmonics* **2006**, *1*, 5–33.
9. Zrazhevskiy, P.; Sena, M.; Gao, X. Designing multifunctional quantum dots for bioimaging, detection, and drug delivery. *Chem. Soc. Rev.* **2010**, *39*, 4326–4354.

10. Bublitz, G.U.; Boxer, S.G. Stark spectroscopy: Applications in chemistry, biology, and materials science. *Annu. Rev. Phys. Chem.* **1997**, *48*, 213–242.

11. Chowdhury, A.; Peteanu, L.A.; Holland, P.L.; Tolman, W.B. The electronic properties of a model active site for blue copper proteins as probed by Stark spectroscopy. *J. Phys. Chem. B* **2002**, *106*, 3007–3012.

12. Ohta, N. Electric field effects on photochemical dynamics in solid films. *Bull. Chem. Soc. Jpn.* **2002**, *75*, 1637–1655.

13. Ohta, N.; Koizumi, M.; Umeuchi, S.; Nishimura, Y.; Yamazaki, I. External electric field effects on fluorescence in an electron donor and acceptor system: Ethylcarbazole and dimethyl terephthalate in PMMA polymer films. *J. Phys. Chem.* **1996**, *100*, 16466–16471.

14. Ohta, N.; Koizumi, M.; Nishimura, Y.; Yamazaki, I.; Tanimoto, Y.; Hatano, Y.; Yamamoto, M.; Kono, H. External electric field effects on fluorescence of methylene-linked D-A systems in polymer films: (Carbazole)–$(CH_2)_n$–(terephthalic acid methyl ester). *J. Phys. Chem.* **1996**, *100*, 19295–19302.

15. Ohta, N.; Mikami, S.; Iwaki, Y.; Tsushima, M.; Imahori, H.; Tamaki, K.; Sakata, Y.; Fukuzumi, S. Acceleration and deceleration of photoinduced electron transfer rates by an electric field in porphyrin-fullerene dyads. *Chem. Phys. Lett.* **2003**, *368*, 230–235.

16. Ohta, N.; Umeuchi, S.; Kanada, T.; Nishimura, Y.; Yamazaki, I. An enhancement of excimer formation rate of pyrene by an external electric field in a PMMA polymer film. *Chem. Phys. Lett.* **1997**, *279*, 215–222.

17. Nakabayashi, T.; Wahadoszamen, M.; Ohta, N. External electric field effects on state energy and photoexcitation dynamics of diphenylpolyenes. *J. Am. Chem. Soc.* **2005**, *127*, 7041–7052.

18. Nakabayashi, T.; Hino, K.; Ohta, Y.; Ito, S.; Nakano, H.; Ohta, N. Electric-field-induced changes in absorption and fluorescence of the green fluorescent protein chromophore in a PMMA film. *J. Phys. Chem. B* **2011**, *115*, 8622–8626.

19. Tayama, J.; Iimori, T.; Ohta, N. Comparative study of electroabsorption spectra of polar and nonpolar organic molecules in solution and in a polymer film. *J. Chem. Phys.* **2009**, *131*, 244509:1–244509:7.

20. Chiang, H.-C.; Iimori, T.; Onodera, T.; Oikawa, H.; Ohta, N. Gigantic electric dipole moment of organic microcrystals evaluated in dispersion liquid with polarized electroabsorption spectra. *J. Phys. Chem. C* **2012**, *116*, 8230–8235.

21. Mehata, M.S.; Hsu, C.-S.; Lee, Y.-P.; Ohta, N. Electric field effects on photoluminescence of polyfluorene thin films: Dependence on excitation wavelength, field strength, and temperature. *J. Phys. Chem. C* **2009**, *113*, 11907–11915.

22. Hsu, H.-Y.; Chiang, H.-C.; Hu, J.-Y.; Awasthi, K.; Mai, C.-L.; Yeh, C.-Y.; Ohta, N.; Diau, E.W.-G. Field-induced fluorescence quenching and enhancement of porphyrin sensitizers on TiO_2 films and in PMMA films. *J. Phys. Chem. C* **2013**, *117*, 24761–24766.

23. Klimov, V.I.; Mikhailovsky, A.A.; Xu, S.; Malko, A.; Hollingsworth, J.A.; Leatherdale, C.A.; Eisler, H.-J.; Bawendi, M.G. Optical gain and stimulated emission in nanocrystal quantum dots. *Science* **2000**, *290*, 314–317.

24. Coe, S.; Woo, W.-K.; Bawendi, M.; Bulović, V. Electroluminescence from single monolayers of nanocrystals in molecular organic devices. *Nature* **2002**, *420*, 800–803.

25. Gur, I.; Fromer, N.A.; Geier, M.L.; Alivisatos, A.P. Air-stable all-inorganic nanocrystal solar cells processed from solution. *Science* **2005**, *310*, 462–465.

26. Colvin, V.L.; Alivisatos, A.P. CdSe nanocrystals with a dipole moment in the first excited state. *J. Chem. Phys.* **1992**, *97*, 730–733.

27. Colvin, V.L.; Cunningham, K.L.; Alivisatos, A.P. Electric field modulation studies of optical absorption in CdSe nanocrystals: Dipolar character of the excited state. *J. Chem. Phys.* **1994**, *101*, 7122–7138.

28. Sacra, A.; Norris, D.J.; Murray, C.B.; Bawendi, M.G. Stark spectroscopy of CdSe nanocrystallites: The significance of transition linewidths. *J. Chem. Phys.* **1995**, *103*, 5236–5245.

29. Ohara, Y.; Nakabayashi, T.; Iwasaki, K.; Torimoto, T.; Ohtani, B.; Ohta, N. Photo-switching behavior of CdS nanoparticles doped in a polymer film. *Comptes Rendus Chim.* **2006**, *9*, 742–749.

30. Ohara, Y.; Nakabayashi, T.; Iwasaki, K.; Torimoto, T.; Ohtani, B.; Hiratani, T.; Konishi, K.; Ohta, N. Electric-field-induced changes in absorption and emission spectra of CdS nanoparticles doped in a polymer film. *J. Phys. Chem. B* **2006**, *110*, 20927–20936.

31. Mehata, M.S.; Majumder, M.; Mallik, B.; Ohta, N. External electric field effects on optical property and excitation dynamics of capped CdS quantum dots embedded in a polymer film. *J. Phys. Chem. C* **2010**, *114*, 15594–15601.

32. Ohshima, R.; Nakabayashi, T.; Kobayashi, Y.; Tamai, N.; Ohta, N. External electric field effects on state energy and photoexcitation dynamics of water soluble CdTe nanoparticles. *J. Phys. Chem. C* **2011**, *115*, 15274–15281.

33. Liu, X.M.; Iimori, T.; Ohshima, R.; Nakabayashi, T.; Ohta, N. Electroabsorption spectra of PbSe nanocrystal quantum dots. *Appl. Phys. Lett.* **2011**, *98*, 161911:1–161911:3.

34. Klem, E.J.D.; Levina, L.; Sargent, E.H. PbS quantum dot electroabsorption modulation across the extended communications band 1200–1700 nm. *Appl. Phys. Lett.* **2005**, *87*, 053101:1–053101:3.

35. Shim, M.; Guyot-Sionnest, P. Permanent dipole moment and charges in colloidal semiconductor quantum dots. *J. Chem. Phys.* **1999**, *111*, 6955–6964.

36. Bawendi, M.G.; Carroll, P.J.; Wilson, W.L.; Brus, L.E. Luminescence properties of CdSe quantum crystallites: Resonance between interior and surface localized states. *J. Chem. Phys.* **1992**, *96*, 946–954.

37. Tsushima, M.; Ushizaka, T.; Ohta, N. Time-resolved measurement system of electrofluorescence spectra. *Rev. Sci. Instrum.* **2004**, *75*, 479–485.

38. Ishikawa, M.; Ye, J.Y.; Maruyama, Y.; Nakatsuka, H. Triphenylmethane dyes revealing heterogeneity of their nanoenvironment: Femtosecond, picosecond, and single-molecule studies. *J. Phys. Chem. A* **1999**, *103*, 4319–4331.

39. Cordero, S.R.; Carson, P.J.; Estabrook, R.A.; Strouse, G.F.; Buratto, S.K. Photo-activated luminescence of CdSe quantum dot monolayers. *J. Phys. Chem. B* **2000**, *104*, 12137–12142.

40. Maenosono, S.; Dushkin, C.D.; Saita, S.; Yamaguchi, Y. Optical memory media based on excitation-time dependent luminescence from a thin film of semiconductor nanocrystals. *Jpn. J. Appl. Phys.* **2000**, *39*, 4006–4012.

41. Underwood, D.F.; Kippeny, T.; Rosenthal, S.J. Ultrafast carrier dynamics in CdSe nanocrystals determined by femtosecond fluorescence upconversion spectroscopy. *J. Phys. Chem. B* **2001**, *105*, 436–443.

42. Jones, M.; Nedeljkovic, J.; Ellingson, R.J.; Nozik, A.J.; Rumbles, G. Photoenhancement of luminescence in colloidal CdSe quantum dot solutions. *J. Phys. Chem. B* **2003**, *107*, 11346–11352.

43. Gurinovich, L.I.; Lyutich, A.A.; Stupak, A.P.; Artem'ev, M.V.; Gaponenko, S.V. Effect of an electric field on photoluminescence of cadmium selenide nanocrystals. *J. Appl. Spectrosc.* **2010**, *77*, 120–125.

44. Yu, W.W.; Qu, L.; Guo, W.; Peng, X. Experimental determination of the extinction coefficient of CdTe, CdSe, and CdS nanocrystals. *Chem. Mater.* **2003**, *15*, 2854–2860.

45. Jalviste, E.; Ohta, N. Stark absorption spectroscopy of indole and 3-methylindole. *J. Chem. Phys.* **2004**, *121*, 4730–4739.